HHS Public Access

Author manuscript

Hepatology. Author manuscript; available in PMC 2019 March 13.

Published in final edited form as:

Hepatology. 2018 February ; 67(2): 736–749. doi:10.1002/hep.29523.

NLRP3 inflammasome driven liver injury and fibrosis: roles of IL-17 and TNF

Alexander Wree[1,2,*], **Matthew D. McGeough**[1,*], **Maria Eugenia Inzaugarat**[2], **Akiko Eguchi**[1], **Susanne Schuster**[1], **Casey D. Johnson**[1], **Carla A. Peña**[1], **Lukas J. Geisler**[2], **Bettina G Papouchado**[3], **Hal M. Hoffman**[1], and **Ariel E. Feldstein**[1]

[1]Department of Pediatrics, University of California – San Diego, La Jolla

[2]Department of Internal Medicine III, RWTH University Hospital Aachen, Germany

[3]Department of Pathology, University of California San Diego, CA, USA

Abstract

The NLRP3 inflammasome, a caspase-1 activation platform plays a key role in the modulation of liver inflammation and fibrosis. Here, we tested the hypothesis that interleukin 17 (IL-17) and tumor necrosis factor (TNF) are key cytokines involved in amplifying and perpetuating the liver damage and fibrosis resulting from NLRP3 activation. To address this hypothesis gain of function *Nlrp3*^{A350V} knock-in mice were bred onto *il17a* and *Tnf* knockout backgrounds allowing for constitutive *Nlrp3* activation in myeloid derived cells in mice deficient in IL-17 or TNF. Livers of *Nlrp3*^{A350V} knock-in mice exhibited severe liver inflammatory changes characterized by infiltration with neutrophils, increased expression of CXCL1 and CXCL2 chemokines, activated inflammatory macrophages and elevated levels of IL-17 and TNF. Mutants with ablation of *il17a* signal showed fewer neutrophils when compared to intact *Nlrp3*^{A350V} mutants, but still significant inflammatory changes when compared to the non-mutant *il17a* knockout littermates. The severe inflammatory changes associated with mutant *Nlrp3* were almost completely rescued by *Tnf* knockout in association with a marked decrease in circulating IL-1β levels. Intact *Nlrp3*^{A350V} mutants showed changes of liver fibrosis, as evidenced by morphometric quantitation of Sirius red staining and increased mRNA levels of profibrotic genes including CTGF and TIMP-1. *Il17a* lacking mutants exhibited amelioration of the aforementioned fibrosis, while *Tnf* deficient mutants showed no signs of fibrosis when compared to littermate controls.

Conclusion—Our study uncovers key roles for TNF, and to a lesser extent IL-17, as mediators of liver inflammation and fibrosis induced by constitutive NLRP3 inflammasome activation in myeloid derived cells. These findings may lead to novel therapeutic strategies aimed at halting the progression of liver injury and fibrogenesis in various liver pathogenesis driven by NLRP3 activation.

Address for correspondence Ariel E. Feldstein, M. D., Professor of Pediatrics, Department of Pediatrics, University of California San Diego, 9500 Gilman Drive, MC 0715, La Jolla, CA. 92037-0715, USA, Tel: + 1 858 966 8907, Fax: + 1 858 966 8917, afeldstein@ucsd.edu.

*Authors contributed equally

Disclosures

HMH is a consultant and speaker for Novartis and SOBI. All other authors state that they have nothing to disclose.

Keywords

NLRP3; inflammation; liver fibrosis; IL17; TNF

Introduction

Inflammation in the absence of infection (sterile inflammation) (SI) has evolved as an important mechanism of liver injury in various acute and chronic liver disorders. (1, 2) SI in the liver is often initiated when damaged hepatocytes, undergoing cell death, expose intracellular molecules that can be recognized by cells of the innate immune system. In particular, resident macrophages or Kupffer cells become activated and trigger an inflammatory response through common pathways involving the NLRP3 inflammasome and interleukin 1 beta (IL-1β). (3, 4) Activation of the NLRP3 inflammasome results in a wide range of immune responses including production of pro-inflammatory cytokines, chemokines with the subsequent recruitment of neutrophils and other immune cells, and cell death.(5, 6) Growing evidence has linked inflammasome-driven inflammation to tissue damage and liver fibrosis in conditions such as drug-induced liver injury, alcoholic steatohepatitis (ASH), and nonalcoholic steatohepatitis (NASH).(7–9)

Recent studies from our lab using constitutively activated *Nlrp3* mutant mice demonstrated that NLRP3 activation is not only required for hepatic inflammation and fibrosis, but is also sufficient to induce programmed inflammatory cell death termed pyroptosis.(10) The present study was conducted to dissect the downstream signals involved in this process and in particular to test the hypothesis that two pathways with growing importance in liver pathology, interleukin 17 (IL-17)(11–17) and tumor necrosis factor (TNF) (18–20), are key in amplifying and perpetuating the liver damage and fibrosis resulting from NLRP3 activation. We approached this hypothesis by breeding unique mouse models that express mutant hyperactive *Nlrp3* in myeloid derived cells in mice that are deficient in IL-17 or TNF and investigate liver inflammation and fibrogenesis in these mice.

Materials and Methods

Mouse Strains

Nlrp3^{A350VneoR} mice were generated as previously described, with an alanine 350 to valine (A350V) substitution and the presence of an intronic floxed neomycin resistance cassette, in which expression of the mutation does not occur unless the *Nlrp3* mutants are first bred with mice expressing Cre recombinase.(21) *Nlrp3*^{A350VneoR} mice were then bred onto *il17a* knockout mice (a gift from Y. Iwakura (University of Tokyo, Tokyo, Japan) and E. Raz (University of California San Diego, La Jolla, CA, US)) - or *Tnf* knockout mice – B6;129S-Tnftm1Gkl/J (TNF$^{-/-}$) mice purchased from Jackson Laboratory (Bar Harbor, ME, US)-background. The resultant mice were further crossed with *il17a* or *Tnf* knockout mice expressing a Cre recombinase under the Lysozyme promoter allowing for mutant *Nlrp3* expression in myeloid derived cells in mice deficient in *il17a* or *Tnf*.(22) Hemozygous Nlrp3 knockout littermates lacking the Cre recombinase were employed as control animals. The experimental protocols were approved by the Institutional Animal Care and Use Committee

at the University of California, San Diego. All efforts were made to minimize pain and distress during animal husbandry and experimental assessments.

In vivo LPS Induction

$Nlrp3^{A350V}$, $Nlrp3^{A350V}Il17^{-/-}$ and $Nlrp3^{A350V}Tnf^{-/-}$ mice were given a single intraperitoneal injection of lipopolysaccharides from Escherichia coli 0127:B8 (Sigma-Aldrich, St. Louis, MO, USA). LPS was injected at a concentration of 25 μg/kg and mice were sacrificed and liver was collected four hours post-injection.

Liver sample preparation

At an age of seven to nine days pups were sacrificed, the peritoneal and thoracic cavities opened, and blood samples were taken via cardiac puncture. Next, using phosphate-buffered saline (PBS), blood was flushed out of the liver via a catheter in the left main cardiac chamber. The livers were harvested and tissue was divided: (i) a representative section was fixed in 10% formalin for 24h and embedded in paraffin, (ii) samples of 50 mg were placed in 500μl of RNAlater® Solution (Life technologies, Carlsbad, CA, USA), (iii) Remaining liver tissue was quickly frozen in liquid nitrogen and stored in −80°C.

Histology, immunohistochemistry and Sirius Red staining

Liver tissues were fixed, embedded in paraffin, and processed on slides for hematoxylin-eosin (H&E) staining. Inflammation was quantified on the basis of the NAFLD activity score (NAS) by an experienced pathologist (Dr. Bettina Papouchado) in routinely stained tissue sections.(23) Liver fibrosis was assessed using Sirius Red, whereby liver sections were incubated for 2 h at room temperature with an aqueous solution of saturated picric acid containing 0.1% Fast Green FCF and 0.1% Direct Red.

Primary monoclonal antibodies used to perform immunostaining were: anti-F4/80 (a murine pan-macrophage marker) (AbDSerotec, Hercules, CA, USA), anti-myeloperoxidase (MPO) (Thermo Scientific, Waltham, MA, USA), anti-Ly6C (Abcam, Cambridge, UK), negative controls has primary antibodies omitted. The specimens were deparaffinized and hydrated in ethanol, the antigens were retrieved in citrate buffer pH 6.0 for 30 minutes at 95°C or treated with 2% BSA 1x Triton in TBS-T for 30 min at room temperature. Following overnight incubation with primary antibodies, horseradish peroxidase (HRP) or Alexa-Fluor 488 conjugated second antibody were applied. For color reaction of HRP, Streptavidin-peroxidase complex 3, 3-diaminobenzidine tetrahydroxychloride was used as chromogen and the slides were counterstained with hematoxylin. All photos were taken by NanoZoomer 2.0HT Slide Scanning System (Hamamatsu, Japan). A total of three fields per sample were examined. The number of MPO-positive cells as well as the F4/80 stained-area per field was determined using ImageJ software (National Institute of Health, USA) (Supplemental Figure 4).

Fluorescence in situ hybridization (FISH)

After deparaffinization and rehydration, the specimens were permeabilized with PBS-0, 3% Triton for 30 min and then, incubated at 72°C for 2 min. Following incubation overnight at

62°C with either TNF or IL17A probe, the slides were washed with hybridization buffer and mounted.

Real-time PCR

Total RNA was isolated from liver tissue and analyzed as previously described.(10) The sequences of the primers used for quantitative PCR are given in supplemental table 1.

Immunoblot analysis and ELISA

Immunoblot analysis was performed as previously described.(24) Anti- IL-17A antibody (Cell Signaling, Danvers, MA, US), anti- TNF-α (abcam, Cambridge, MA, US), and anti-α-SMA (GeneTex, Irvine, CA, USA) antibodies were used in combination with appropriate peroxidase-conjugated secondary antibodies. Protein load was verified with GAPDH antibody (Genetex, Irvine, CA) or α-tubulin antibody (dilution 1:10,000) (Hybridomabank, University of Iowa) (kindly provided by M. Kaulich, University of California San Diego, La Jolla, CA, US). Bands were visualized with the enhanced chemiluminescence reagent and digitized using a CCD camera (ChemiDoc®, Biorad, Hercules, CA, USA). Expression intensity was quantified by ImageLab (Biorad). Quantification of serum IL-1β levels were performed according to the manufactures' instruction (R&D Systems, Minneapolis, MN, USA).

Unless stated otherwise, all other chemicals were purchased from Sigma-Aldrich (St. Louis, MO, USA).

FACS analysis

Whole livers were force filtered through a 70μm nylon cell strainer (BD) with PBS. The solution was centrifuged for 1min at 8°C with 500rpm producing a pellet of parenchymal cells and a supernatant incorporating the infiltrating cells. Infiltrating cells were classified by multicolour analysis after incubation with CD11b (eBioscience, San Diego, CA, USA), F4/80 (AbD serotec, Kidlington, UK) and Ly6G (eBioscience) for 30min on ice and washed with 3% FBS-PBS. For analysis of intracellular production of TNF and IL17A, cells were further permeabilized and incubated with TNF (eBioscience) or IL17 (eBiosicence) antibodies. Cells were analyzed by flow cytometry (BD LRS II).

Statistical analyses

Analyses were performed with Graph Pad (version 5.03; Graph Pad, Graph Pad Software Inc., CA, USA). The significance level was set at $\alpha = 5\%$ for all comparisons. Data were evaluated using Kruskall-Wallis test and Dunn's Multiple Comparison Test. For group comparisons, we limit this to three comparisons that are of particular interest: Control vs. $Nlrp3^{A350V}$, $Nlrp3^{A350V}$ vs. $Nlrp3^{A350V}/il17a^{-/-}$, and $Nlrp3^{A350V}$ vs. $Nlrp3^{A350V}/Tnf^{-/-}$. Unless otherwise stated, data are expressed as mean +/− SEM or as absolute number or percentage for categorical variables.

Results

Liver inflammation in *Nlrp3*^{A350V} mice is associated with increase in TNF and IL-17

Mice expressing the Nlrp3^{A350V} mutation under the control of the lysozyme promoter exhibited severe liver inflammation (Fig. 1A). Further histological analysis and immunohistochemical staining revealed an increase in neutrophils staining positive for MPO (Fig. 1C). In addition, livers of *Nlrp3*^{A350V} mice displayed elevated numbers of macrophages with activated inflammatory macrophages being the dominant additional cell type, evidenced by high expression of F4/80 and Ly6C (Fig. 1C). As TNF and IL-17 are both known to be increased in several models of liver injury and have been increasingly linked to liver inflammation and fibrogenesis(11, 20), we next assessed their levels in the livers of *Nlrp3*^{A350V} mice. Interestingly, mRNA levels of *Tnf* in the liver of *Nlrp3*^{A350V} mice were increased 10 fold when compared to non-mutant littermates. Hepatic mRNA levels of *Il17a* were also significantly increased (5-fold, $p<0.05$) in *Nlrp3*^{A350V} mice when compared to control animals (Fig. 1B). In line with these changes, protein levels of TNF, the non-biologically active monomerized form (17kDa) as well as the biologically active homotrimer (52kDa),(25) were significantly increased in livers of *Nlrp3* mutant mice (4-fold, $p<0.05$) (Fig. 1D). Protein levels of IL-17A were also found to be increased in *Nlrp3*^{A350V} mice when compared to controls (3-fold, $p<0.05$) (Fig 1D). FISH staining showed a strong expression of TNF in portal track infiltration sites and IL17A in inflammatory foci (Fig 1H), indicating that infiltrating cells are the main source responsible for the production of these cytokines. Flow cytometry analysis revealed that Nlrp3 ^{A350V} mice have increase TNF-producing $CD11b^{+}Ly6G^{-}$ cells (2-fold, $p<0.01$) as well as TNF-producing $CD11b^{+}Ly6G^{+}$ cells (1.5-fold, $p<0.05$) compared to controls (Fig 1G). We also investigated whether other proinflammatory and profibrotic cytokines or chemokines were also upregulated in *Nlrp3*^{A350V} mice. Increased hepatic mRNA levels of IL-1β (5-fold, $p<0.05$), IL-33 (3-fold, $p<0.05$) as well as MCP-1 (4-fold, $p<0.05$) were observed in mutant mice when compared to controls, while no change was found in mRNA levels of IL-6 and IL-18 (Fig. 1E). *Nlrp3*^{A350V} mice showed increased protein levels of mature IL-1β and IL18 as measure by western blot (Fig. 1F).

TNF but not IL-17 ameliorates Nlrp3 dependent liver inflammation

Based on the increase levels of TNF and IL-17A in the livers of *Nlrp3*^{A350V} mice, we next sought to investigate their role on the liver phenotype resulting from NLRP3 activation. Therefore, we crossed our *Nlrp3*^{A350V} mice with mice globally deficient for *Tnf* or *Il17a* generating mice that exhibit mutant *Nlrp3* expression in myeloid derived cells, but were globally deficient in *Il17a* or *Tnf*. We included seven animals per group and sacrificed them at day nine of age (Supplemental table 2). Control mice exhibited an average body weight of 4.4g (range 3.4g to 5.2g), while *Nlrp3*^{A350V} mice were significantly smaller (1.8g, range 1.6g to 2.2g). *Nlrp3* mutant mice deficient for *il17a* also showed a reduced body weight when compared to *il17a* knockout mice, while *Nlrp3* mutant mice deficient for *Tnf* were indistinguishable from *Tnf* knockout mice (Supplemental table 2). Analysis of liver weight revealed a significant increase in liver weight per body weight in *Nlrp3*^{A350V} mice when compared to control mice (Supplemental table 2, Fig. 2B). This increase was also documented in *Nlrp3*^{A350V}*Il17a*$^{-/-}$ mice when compared to *Il17a*$^{-/-}$ mice, while liver to

body weight ratio was similar in *Nlrp3*^{A350V}*Tnf*$^{-/-}$ and *Tnf*$^{-/-}$ mice (Supplemental table 2, Fig. 2B). Examination of liver histology revealed strong inflammation in *Nlrp3*^{A350V} mice (grade 3) and *Nlrp3*^{A350V}*Il17a*$^{-/-}$ mice (grade 3), while *Nlrp3*^{A350V}*Tnf*$^{-/-}$ mice only showed mild inflammatory changes (grade 1) (Fig. 2A, C). Analysis of serum IL-1β levels revealed a significant increase in in *Nlrp3*^{A350V} mice when compared to control mice (Fig. 2D). Increased serum IL-1β levels were also present in *Nlrp3*^{A350V}*Il17a*$^{-/-}$ mice when compared to *Il17a*$^{-/-}$ mice, while levels in Nlrp3^{A350V} *Tnf*$^{-/-}$ and *Tnf*$^{-/-}$mice were significantly reduced when compared to *Nlrp3*^{A350V} mice (Fig. 2D).

Infiltration with neutrophils and inflammatory macrophages in *Nlrp3* mutant mice depends on TNF signaling

As hepatic infiltration with neutrophils and inflammatory macrophages are prominent in *Nlrp3*^{A350V} mice we next investigated these events in the combined knock-in knockout mice. Immunohistochemistry of liver sections showed higher numbers of MPO positive cells in *Nlrp3*^{A350V} when compared to control mice. *Nlrp3*^{A350V}*Il17a*$^{-/-}$ livers exhibit significant fewer amount of MPO cells while the number of positive cells in *Nlrp3*^{A350V} TNF$^{-/-}$ mice was not different from TNF$^{-/-}$ mice (Fig. 3A, B). In line with this, mRNA levels of MPO were increased by 20-fold in *Nlrp3*^{A350V} mice when compared to control mice; levels in *Nlrp3*^{A350V}*Il17a*$^{-/-}$mice were still increased 5-fold, and levels in *Nlrp3*^{A350V}*Tnf*$^{-/-}$mice were not increased (Fig. 3B). As neutrophilic infiltration as a consequence of NLRP3 activation is mediated in part via a chemokine gradient,(26) we next quantified mRNA levels of CXCL1 and CXCL2, two key chemokines involved in this process in livers of mice from the various experimental groups. We found a marked increase in *Nlrp3*^{A350V} mice (20-fold for CXCL1 and 30-fold for CXCL2) when compared to control animals (Fig. 4C). This increase was also present in *Nlrp3*^{A350V}*Il17a*$^{-/-}$mice (10-fold for CXCL1 and CXCL2). A significant decrease of CXCL1 and CXCL2 expression was observed in *Nlrp3*^{A350V}*Tnf*$^{-/-}$ mice when compared to *Nlrp3*^{A350V} mice (Fig. 4C). Interestingly, pro-IL-1beta mRNA levels were still upregulated in both *Nlrp3*^{A350V}*Tnf*$^{-/-}$ mice (3-fold) and *Nlrp3*^{A350V}*Il17a*$^{-/-}$ mice (3-fold) compared to control mice (Fig 3D), while all groups of mice displayed similar IL-6 (Fig 3E), IL-33 (Fig 3F) and pro-IL18 (Fig 3G) mRNA levels. However, protein levels of pro-IL1β and pro-IL18 as well as mature IL-1β and IL-18 were higher only in *Nlrp3*^{A350V}*Il17a*$^{-/-}$ but not in *Nlrp3*^{A350V}*Tnf*$^{-/-}$ mice (Fig. 3H).

Analysis of hepatic macrophages by immunohistochemistry revealed increased areas of F4/80 and levels of F4/80 mRNA in *Nlrp3*^{A350V} mice (6-fold, $p<0.05$) when compared to control animals and unchanged levels in all other groups of mice (Fig. 4A, B). However, further investigations in macrophage phenotype uncovered a significant increase in inflammatory macrophages as demonstrated by lymphocyte antigen 6 complex (Ly6-c) positive quantification in *Nlrp3*^{A350V} mice and *Nlrp3*^{A350V}*Il17a*$^{-/-}$mice with no detectable increase in *Nlrp3*^{A350V}*Tnf*$^{-/-}$ mice when compared to control mice (Fig. 4C). Surprisingly, CD68 mRNA levels were upregulated only in *Nlrp3*^{A350V}*Il17a*$^{-/-}$ mice but not in *Nlrp3*^{A350V} or *Nlrp3*^{A350V}*Tnf*$^{-/-}$ mice. (Fig. 4D) Further supporting the pro-inflammatory phenotype of macrophages in the livers of *Nlrp3*^{A350V} mice and *Nlrp3*^{A350V}*Il17a*$^{-/-}$mice, mRNA levels of iNOS (inducible form of nitric oxide synthase) and TNF were found to be

increased in both groups. iNOS mRNA levels were found unchanged in *Nlrp3*^{A350V} TNF$^{-/-}$ mice (Fig. 4E, F).

TNF but not IL-17 prevents hepatic stellate cell activation in Nlrp3 mutant mice

Liver inflammation and chronic infiltration with inflammatory macrophages is closely correlated to the activation of hepatic stellate cells (HSCs) and the development of liver fibrosis.(27) Liver sections were therefore stained with Sirius red to assess collagen deposition (Fig. 5A). As expected, positive Sirius red staining was detectable in liver sections of control mice, *Il17a*$^{-/-}$ mice, and *Tnf*$^{-/-}$ mice only in close proximity of the portal field (Fig. 5A). Liver sections of *Nlrp3*^{A350V} and *Nlrp3*^{A350V}*Il17a*$^{-/-}$ mice exhibited bridging fibrosis, while liver sections of *Nlrp3*^{A350V}*Tnf*$^{-/-}$ mice did not show increased collagen deposition. The mRNA levels of connective tissue growth factor (ctgf) (Fig. 5B), tissue inhibitor of matrix metalloproteinase 1 (timp1) (Fig. 5C), and alpha smooth muscle actin (α-SMA) (Fig. 5D) were increased in livers of *Nlrp3*^{A350V} and *Nlrp3*^{A350V}*Il17a*$^{-/-}$ mice, while levels in *Nlrp3*^{A350V}*Tnf*$^{-/-}$ mice did not differ from controls. In line with this, protein levels of α-SMA were also increased in *Nlrp3*^{A350V} and *Nlrp3*^{A350V}*Il17a*$^{-/-}$mice when compared to their corresponding control animals with no difference in *Nlrp3*^{A350V}*Tnf*$^{-/-}$ and *Tnf*$^{-/-}$ mice (Fig. 5E).

LPS-driven liver damage is ameliorated by TNF but not IL17 in Nlrp3 mutant mice

In order to further evaluate the involvement of TNF and IL17 in NLRP3 mediated liver damage, we challenged the different group of mice with an inflammatory stimulus. We injected LPS intraperitoneally and observed the liver damage after 4 hours. Liver histology revealed strong inflammation in *Nlrp3*^{A350V} mice (grade 2) as well as *Nlrp3*^{A350V}*Il17a*$^{-/-}$ mice (grade 3), while *Nlrp3*^{A350V}*Tnf*$^{-/-}$ mice showed no signs of inflammatory changes (grade 0) (Fig. 6A, B). Immunohistochemistry of liver sections displayed extensive MPO positive cells infiltration (Fig. 6A, C) along with the presence of high number of F4/80 macrophages (Fig 6A, D) in *Nlrp3*^{A350V} and *Nlrp3*^{A350V}*Il17a*$^{-/-}$. Liver sections of *Nlrp3*^{A350V}*Tn* f$^{-/-}$ mice displayed fewer number of MPO infiltrating positive cells (Fig 6A, C) as well as decreased amount of F4/80 positive cells (Fig 6A, D).

Discussion

The key findings of the present study provide new information about the downstream pathways involved in the development of liver inflammation and fibrogenesis associated with myeloid cell specific NLRP3 activation. Our results demonstrate that the levels of both TNF and IL-17, two key cytokines linked to liver pathology, are increased in the livers of mice with constitutively activated *Nlrp3* in myeloid derived cells. TNF signaling but not IL-17 appears to be crucial in triggering liver inflammation, neutrophils and pro-inflammatory macrophage recruitment, as well as in activation of fibrogenic pathways that are central to the development of liver fibrosis.

Emerging evidence supports a central role of NLRP3 Inflammasome in the pathogenesis of many liver diseases including alcoholic and nonalcoholic fatty liver disease (NAFLD) as well as liver fibrosis.(24, 28–31) Indeed, studies using global knockout mice of different

inflammasome components, or pharmacological inhibitors of IL-1β signaling, have suggested protective effects of NLRP3 signaling suppression in liver injury and fibrotic changes associated with these conditions.(28) IL-1β signaling appears to be an important contributor for the liver changes resulting from NLRP3 activation. However, our previous results indicate that IL-1-independent pathways also play an important role as treatment with an interleukin-1 receptor antagonist (anakinra) only partially attenuated liver inflammation, whereas fibrogenesis was unchanged.(10) Additionally, deletion of the Interleukin 18 (IL-18) receptor in *Nlrp3* knockin mice resulted in partial phenotypic rescue that abolished skin and visceral disease in young mice and normalized serum cytokines to a greater extent than breeding to Interleukin 1 receptor knockout mice.(32) Significant systemic inflammation developed in aging *Nlrp3* mutant IL-18 receptor knockout mice, suggesting that IL-1β and IL-18 drive pathology at different stages of the disease process.(32) The current study was conducted to further dissect the downstream events that may amplify and perpetuate the inflammatory responses and contribute to activation of HSCs, a central event in liver fibrosis.(33) We focused on IL-17 and TNF, two pathways that have been increasingly linked to liver injury, particular in the context of NAFLD and alcoholic liver disease. While IL-17 production can be regulated via NLRP3 activation,(34–36) TNF production is mainly thought to occur via signals that lead to activation of NFkB. (37, 38) NLRP3 activation may amplify this production in an autocrine or paracrine fashion by inducing the maturation and release of IL-1β and IL-18, which then interact with their own membrane receptors.(39, 40) Furthermore, both cytokines have been involved in creating an autoinflammatory loop that characterizes these disorders,(41) while IL-17 is an important contributor for tissue recruitment of neutrophils, a central feature found in the livers of mice with constitutive active NLRP3.

Our results demonstrate that NLRP3 inflammasome induced liver inflammation and liver fibrogenesis are influenced by IL-17 and TNF, with TNF having more prominent effect (Fig. 5F). The expression of both cytokines was increased in the livers of Nlrp3 mutant mice. Studies using FISH and FACS analysis demonstrated the infiltrating inflammatory cells are the main source for these cytokines. The unexpected significance of TNF ablation in *Nlrp3* mutant mice could be explained by a feedback loop with IL-1β as reported by Tangi et al. The authors showed an increase in IL-1β mRNA and protein levels in cell culture supernatants of aortic smooth muscle cells upon stimulation with TNF that was dependent on NLRP3 signaling. (42). Consistent with this, our current data demonstrate a significant reduction of IL-1β levels in *Nlrp3* mutants in the absence of TNF. Due to the important role for IL-17 in recruitment of neutrophils to the liver and its role in the context of liver fibrosis and activation of HSCs, we expected a major beneficial effect of IL-17 ablation on liver disease in our *Nlrp3* gain-of-function model.(14, 16). Surprisingly, we observed only a slight reduction in neutrophilic infiltration by IL-17 ablation. These finding suggest that the inflammatory environment generated by NLRP3 activation and the recruitment of circulating neutrophils occur by parallel redundant pathways, which may explain the only minimal protective effects on the development of liver fibrosis observed in our mutant mice.

Although the role of TNF and its inhibition in animal models of liver injury offered encouraging therapeutic perspectives, targeting this cytokine for the treatment of human liver diseases remains uncertain.(43) Indeed, extensive evidence from animal models on

various liver disorders such nonalcoholic and alcoholic liver disease have demonstrated a central role for TNF in development of liver injury and modulation of disease severity. Treatment of leptin deficient *ob/ob* mice with anti-TNF antibodies improves NASH and hepatic insulin resistance.(44) Mice genetically deficient in TNF type 1 receptor (TNFR1) are resistant to steatosis and liver injury induced by high caloric diets as well as alcohol exposure.(45–47) Our current results also suggest the potential beneficial effects of modulating TNF signaling in the context of NLRP3 driven liver pathology. In humans, various molecules that target TNF such as pentoxifylline, etanercept, (a fusion protein that acts as a "decoy receptor" for TNF) as well as the various anti-TNF monoclonal antibodies currently available for clinical use, have been proposed as potential therapy for the treatment of liver disease. Early studies using pentoxifylline, a weak TNF inhibitor, have shown positive results with diminished serum levels of aminotransferases and improved inflammation and fibrosis in patients with NASH.(48) However, caution must be taken as a randomized placebo-controlled trial using etanercept was associated with a significantly higher mortality rate in patients with moderate-to-severe acute alcoholic hepatitis, an effect that was mainly attributed to an increased rate of severe infections.(49)

In summary, our current study reveals key roles for TNF, and to a lesser extent IL-17, as mediators of liver inflammation and fibrosis induced by constitutive NLRP3 inflammasome activation in myeloid derived cells. These findings may lead to novel therapeutic strategies aimed at halting the progression of liver injury and fibrogenesis in various liver pathologies driven by NLRP3 activation.

Supplementary Material

Refer to Web version on PubMed Central for supplementary material.

Acknowledgments

This work used the facilities of the UCSD Microscopy Core supported by the UCSD Neuroscience Microscopy Shared Facility grant (P30 NS047101). We thank Dr. Lori Broderick for editorial insights.

Funding

The work was funded by NIH (DK076852 and DK082451 to AEF and AI52430 to HMH), German Research Foundation (DFG-grant WR173/2-1 and SFB/TRR 57 to AW), and START-Program of the Faculty of Medicine, RWTH Aachen to AW).

Abbreviations

α-SMA	alpha smooth muscle actin
ASC	apoptosis-associated speck-like protein containing a caspase recruitment domain
CARD	caspase recruitment domain-containing protein 8
CLD	chronic liver disease
CTGF	connective tissue growth factor

CXCL	chemokine (C-X-C motif) ligand
F4/80	murine macrophage marker
HSC	hepatic stellate cell
IL	interleukin
iNOS	inducible form of nitric oxide synthase
MPO	myeloperoxidase
NAS	nonalcoholic fatty liver disease activity score
NLRs	nucleotide-binding oligomerization domain (NOD) leucine-rich repeat containing receptors
SI	sterile inflammation
TIMP1	tissue inhibitor of matrix metalloproteinase 1
TNF	tumor necrosis factor.

References

1. Hoque R, Farooq A, Mehal WZ. Sterile inflammation in the liver and pancreas. J Gastroenterol Hepatol. 2013; (28 Suppl 1):61–67. [PubMed: 23855298]
2. Kubes P, Mehal WZ. Sterile inflammation in the liver. Gastroenterology. 2012; 143:1158–1172. [PubMed: 22982943]
3. Matzinger P. Tolerance, danger, and the extended family. Annu Rev Immunol. 1994; 12:991–1045. [PubMed: 8011301]
4. Rock KL, Latz E, Ontiveros F, Kono H. The sterile inflammatory response. Annu Rev Immunol. 2010; 28:321–342. [PubMed: 20307211]
5. Wree A, Broderick L, Canbay A, Hoffman HM, Feldstein AE. From NAFLD to NASH to cirrhosis-new insights into disease mechanisms. Nat Rev Gastroenterol Hepatol. 2013; 10:627–636. [PubMed: 23958599]
6. Broderick L, De Nardo D, Franklin BS, Hoffman HM, Latz E. The Inflammasome and Autoinflammatory Syndromes. Annu Rev Pathol. 2014
7. Maher JJ. DAMPs ramp up drug toxicity. J Clin Invest. 2009; 119:246–249. [PubMed: 19244605]
8. Gao B, Seki E, Brenner DA, Friedman S, Cohen JI, Nagy L, Szabo G, et al. Innate immunity in alcoholic liver disease. Am J Physiol Gastrointest Liver Physiol. 2011; 300:G516–525. [PubMed: 21252049]
9. Brenner DA, Seki E, Taura K, Kisseleva T, Deminicis S, Iwaisako K, Inokuchi S, et al. Non-alcoholic steatohepatitis-induced fibrosis: Toll-like receptors, reactive oxygen species and Jun N-terminal kinase. Hepatol Res. 2011; 41:683–686. [PubMed: 21711427]
10. Wree A, Eguchi A, McGeough MD, Pena CA, Johnson CD, Canbay A, Hoffman HM, et al. NLRP3 inflammasome activation results in hepatocyte pyroptosis, liver inflammation and fibrosis. Hepatology. 2013
11. Hammerich L, Heymann F, Tacke F. Role of IL-17 and Th17 cells in liver diseases. Clin Dev Immunol. 2011; 2011:345803. [PubMed: 21197451]
12. Veldhoen M, Hocking RJ, Atkins CJ, Locksley RM, Stockinger B. TGFbeta in the context of an inflammatory cytokine milieu supports de novo differentiation of IL-17-producing T cells. Immunity. 2006; 24:179–189. [PubMed: 16473830]

13. Lemmers A, Moreno C, Gustot T, Marechal R, Degre D, Demetter P, de Nadai P, et al. The interleukin-17 pathway is involved in human alcoholic liver disease. Hepatology. 2009; 49:646–657. [PubMed: 19177575]
14. Meng F, Wang K, Aoyama T, Grivennikov SI, Paik Y, Scholten D, Cong M, et al. Interleukin-17 signaling in inflammatory, Kupffer cells, and hepatic stellate cells exacerbates liver fibrosis in mice. Gastroenterology. 2012; 143:765–776. e761–763. [PubMed: 22687286]
15. Zhang JY, Zhang Z, Lin F, Zou ZS, Xu RN, Jin L, Fu JL, et al. Interleukin-17-producing CD4(+) T cells increase with severity of liver damage in patients with chronic hepatitis B. Hepatology. 2010; 51:81–91. [PubMed: 19842207]
16. Hara M, Kono H, Furuya S, Hirayama K, Tsuchiya M, Fujii H. Interleukin-17A plays a pivotal role in cholestatic liver fibrosis in mice. J Surg Res. 2013; 183:574–582. [PubMed: 23578751]
17. Yasumi Y, Takikawa Y, Endo R, Suzuki K. Interleukin-17 as a new marker of severity of acute hepatic injury. Hepatol Res. 2007; 37:248–254. [PubMed: 17397512]
18. Bieghs V, Trautwein C. The innate immune response during liver inflammation and metabolic disease. Trends Immunol. 2013; 34:446–452. [PubMed: 23668977]
19. Schwabe RF, Brenner DA. Mechanisms of Liver Injury. I. TNF-alpha-induced liver injury: role of IKK, JNK, and ROS pathways. Am J Physiol Gastrointest Liver Physiol. 2006; 290:G583–589. [PubMed: 16537970]
20. Tacke F, Luedde T, Trautwein C. Inflammatory pathways in liver homeostasis and liver injury. Clin Rev Allergy Immunol. 2009; 36:4–12. [PubMed: 18600481]
21. Brydges SD, Mueller JL, McGeough MD, Pena CA, Misaghi A, Gandhi C, Putnam CD, et al. Inflammasome-mediated disease animal models reveal roles for innate but not adaptive immunity. Immunity. 2009; 30:875–887. [PubMed: 19501000]
22. Clausen BE, Burkhardt C, Reith W, Renkawitz R, Forster I. Conditional gene targeting in macrophages and granulocytes using LysMcre mice. Transgenic research. 1999; 8:265–277. [PubMed: 10621974]
23. Kleiner DE, Brunt EM, Van Natta M, Behling C, Contos MJ, Cummings OW, Ferrell LD, et al. Design and validation of a histological scoring system for nonalcoholic fatty liver disease. Hepatology. 2005; 41:1313–1321. [PubMed: 15915461]
24. Wree A, McGeough MD, Pena CA, Schlattjan M, Li H, Inzaugarat ME, Messer K, et al. NLRP3 inflammasome activation is required for fibrosis development in NAFLD. J Mol Med (Berl). 2014
25. Smith RA, Baglioni C. The active form of tumor necrosis factor is a trimer. J Biol Chem. 1987; 262:6951–6954. [PubMed: 3034874]
26. McDonald B, Pittman K, Menezes GB, Hirota SA, Slaba I, Waterhouse CC, Beck PL, et al. Intravascular danger signals guide neutrophils to sites of sterile inflammation. Science. 2010; 330:362–366. [PubMed: 20947763]
27. Puche JE, Saiman Y, Friedman SL. Hepatic stellate cells and liver fibrosis. Compr Physiol. 2013; 3:1473–1492. [PubMed: 24265236]
28. Petrasek J, Bala S, Csak T, Lippai D, Kodys K, Menashy V, Barrieau M, et al. IL-1 receptor antagonist ameliorates inflammasome-dependent alcoholic steatohepatitis in mice. J Clin Invest. 2012; 122:3476–3489. [PubMed: 22945633]
29. Dixon LJ, Flask CA, Papouchado BG, Feldstein AE, Nagy LE. Caspase-1 as a central regulator of high fat diet-induced non-alcoholic steatohepatitis. PLoS One. 2013; 8:e56100. [PubMed: 23409132]
30. Dixon LJ, Berk M, Thapaliya S, Papouchado BG, Feldstein AE. Caspase-1-mediated regulation of fibrogenesis in diet-induced steatohepatitis. Lab Invest. 2012; 92:713–723. [PubMed: 22411067]
31. Szabo G, Csak T. Inflammasomes in liver diseases. Journal of hepatology. 2012; 57:642–654. [PubMed: 22634126]
32. Brydges SD, Broderick L, McGeough MD, Pena CA, Mueller JL, Hoffman HM. Divergence of IL-1, IL-18, and cell death in NLRP3 inflammasomopathies. J Clin Invest. 2013
33. Friedman SL. Mechanisms of hepatic fibrogenesis. Gastroenterology. 2008; 134:1655–1669. [PubMed: 18471545]

34. Maher BM, Mulcahy ME, Murphy AG, Wilk M, O'Keeffe KM, Geoghegan JA, Lavelle EC, et al. Nlrp-3 driven IL-17 production by gammadelta T-cells controls infection outcomes during Staphylococcus aureus surgical site infection. Infect Immun. 2013
35. Bruchard M, Mignot G, Derangere V, Chalmin F, Chevriaux A, Vegran F, Boireau W, et al. Chemotherapy-triggered cathepsin B release in myeloid-derived suppressor cells activates the Nlrp3 inflammasome and promotes tumor growth. Nat Med. 2013; 19:57–64. [PubMed: 23202296]
36. Sutton CE, Lalor SJ, Sweeney CM, Brereton CF, Lavelle EC, Mills KH. Interleukin-1 and IL-23 induce innate IL-17 production from gammadelta T cells, amplifying Th17 responses and autoimmunity. Immunity. 2009; 31:331–341. [PubMed: 19682929]
37. Yao J, Mackman N, Edgington TS, Fan ST. Lipopolysaccharide induction of the tumor necrosis factor-alpha promoter in human monocytic cells. Regulation by Egr-1, c-Jun, and NF-kappaB transcription factors. J Biol Chem. 1997; 272:17795–17801. [PubMed: 9211933]
38. Bohuslav J, Kravchenko VV, Parry GC, Erlich JH, Gerondakis S, Mackman N, Ulevitch RJ. Regulation of an essential innate immune response by the p50 subunit of NF-kappaB. J Clin Invest. 1998; 102:1645–1652. [PubMed: 9802878]
39. Franchi L, Eigenbrod T, Nunez G. Cutting edge: TNF-alpha mediates sensitization to ATP and silica via the NLRP3 inflammasome in the absence of microbial stimulation. J Immunol. 2009; 183:792–796. [PubMed: 19542372]
40. Paramel GV, Sirsjo A, Fransen K. Role of genetic alterations in the NLRP3 and CARD8 genes in health and disease. Mediators Inflamm. 2015; 2015:846782. [PubMed: 25788762]
41. Grine L, Dejager L, Libert C, Vandenbroucke RE. An inflammatory triangle in psoriasis: TNF, type I IFNs and IL-17. Cytokine Growth Factor Rev. 2015; 26:25–33. [PubMed: 25434285]
42. Tangi TN, Elmabsout AA, Bengtsson T, Sirsjo A, Fransen K. Role of NLRP3 and CARD8 in the regulation of TNF-alpha induced IL-1beta release in vascular smooth muscle cells. Int J Mol Med. 2012; 30:697–702. [PubMed: 22711073]
43. Braunersreuther V, Viviani GL, Mach F, Montecucco F. Role of cytokines and chemokines in non-alcoholic fatty liver disease. World J Gastroenterol. 2012; 18:727–735. [PubMed: 22371632]
44. Li Z, Yang S, Lin H, Huang J, Watkins PA, Moser AB, Desimone C, et al. Probiotics and antibodies to TNF inhibit inflammatory activity and improve nonalcoholic fatty liver disease. Hepatology. 2003; 37:343–350. [PubMed: 12540784]
45. Feldstein AE, Canbay A, Guicciardi ME, Higuchi H, Bronk SF, Gores GJ. Diet associated hepatic steatosis sensitizes to Fas mediated liver injury in mice. J Hepatol. 2003; 39:978–983. [PubMed: 14642615]
46. Tomita K, Tamiya G, Ando S, Ohsumi K, Chiyo T, Mizutani A, Kitamura N, et al. Tumour necrosis factor alpha signalling through activation of Kupffer cells plays an essential role in liver fibrosis of non-alcoholic steatohepatitis in mice. Gut. 2006; 55:415–424. [PubMed: 16174657]
47. Yin M, Wheeler MD, Kono H, Bradford BU, Gallucci RM, Luster MI, Thurman RG. Essential role of tumor necrosis factor alpha in alcohol-induced liver injury in mice. Gastroenterology. 1999; 117:942–952. [PubMed: 10500078]
48. Lee YM, Sutedja DS, Wai CT, Dan YY, Aung MO, Zhou L, Cheng CL, et al. A randomized controlled pilot study of Pentoxifylline in patients with non-alcoholic steatohepatitis (NASH). Hepatol Int. 2008; 2:196–201. [PubMed: 19669304]
49. Boetticher NC, Peine CJ, Kwo P, Abrams GA, Patel T, Aqel B, Boardman L, et al. A randomized, double-blinded, placebo-controlled multicenter trial of etanercept in the treatment of alcoholic hepatitis. Gastroenterology. 2008; 135:1953–1960. [PubMed: 18848937]

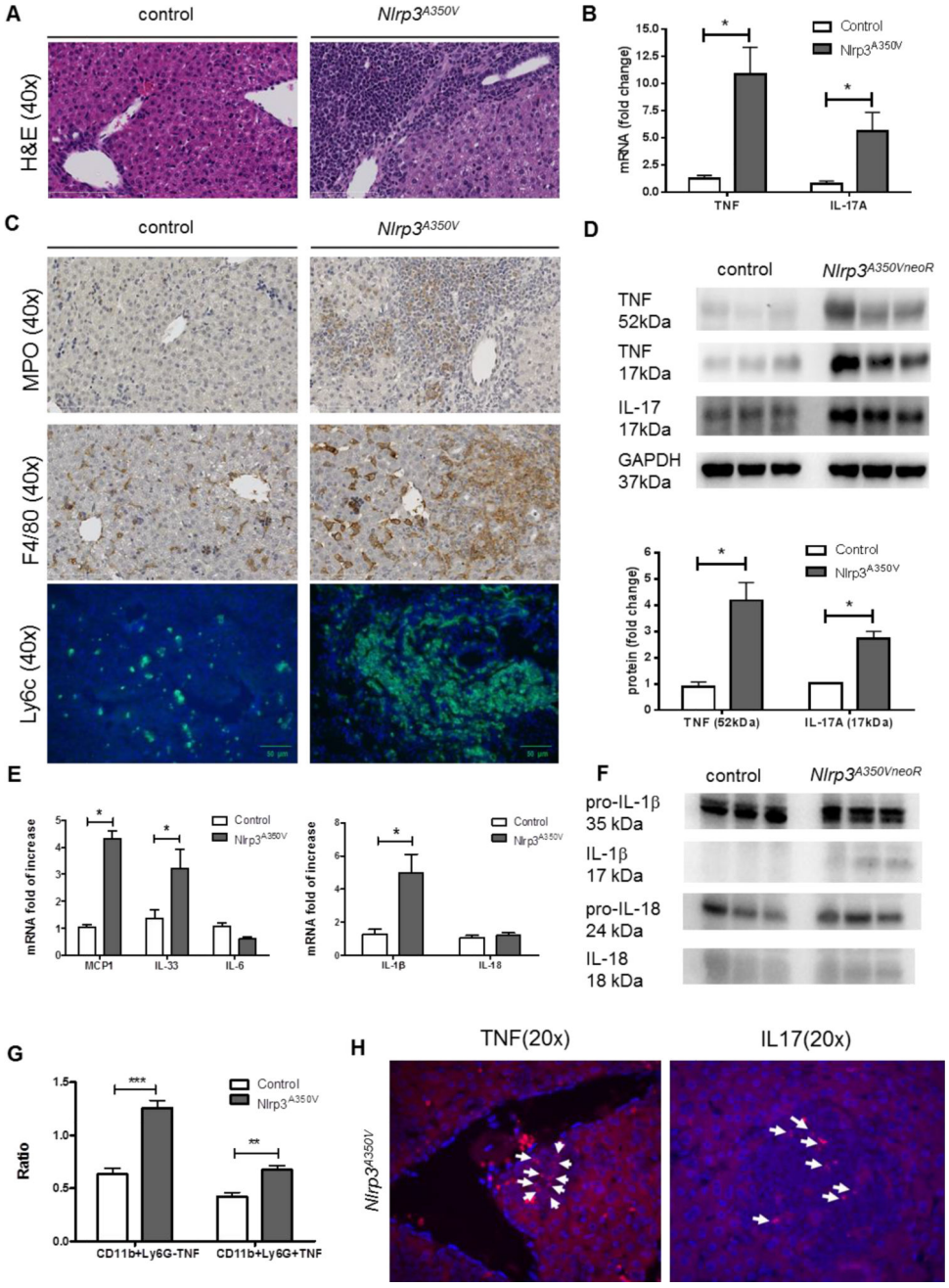

Figure 1. Evidence of IL17 and TNF in *Nlrp3* mutant mice

Nlrp3^{A350V} mice exhibited severe liver inflammation (A). mRNA levels of TNF and IL-17 were increased in *Nlrp3*^{A350V} mice when compared to control mice (B) Detection of myeloperoxidase (MPO, neutrophils), F4/80 (murine pan-macrophage marker) as well as lymphocyte antigen 6 complex (Ly6C) (activated macrophages) positive cells in liver of *Nlrp3*^{A350V} mice (C). Protein levels of TNF monomer (17kDa), trimeric TNF (52kDa), and IL-17A were increased in liver samples of *Nlrp3*^{A350V} mice when compared to control mice (D). MCP-1, IL-33 as well as IL-1β mRNA levels were upregulated in *Nlrp3*^{A350V} mice when compared to control mice, while IL-6 and IL-18 mRNA levels were similar between

both groups (E) Mature IL-1β (17kDa) as well as mature IL-18 (18kDa) but not pro-IL1β (35kDa) or pro-IL18 (24kDa) protein levels were increased in liver samples of Nlrp3^{A350V} mice when compared to control mice (F). Flow cytometry analysis showed that *Nlrp3*^{A350V} mice have increase TNF-producing CD11b+Ly6G− cells as well as TNF-producing CD11b +Ly6G+ cells compared to controls (G). FISH staining showed a strong expression of TNF in portal track infiltration sites and IL17A in inflammatory foci (H). (* = $p<0.05$, ** = $p<0.01$, = $p<0.001$)

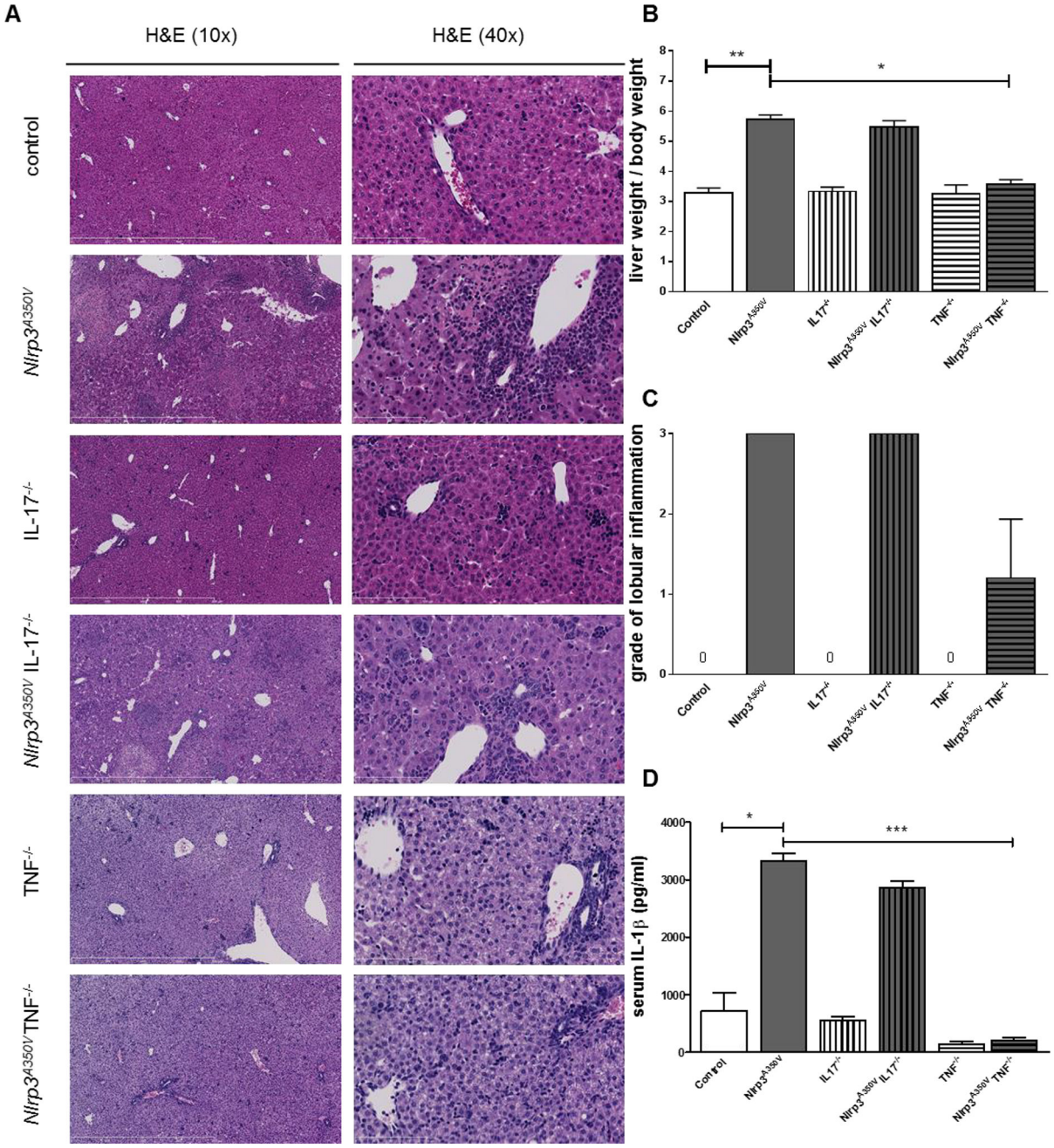

Figure 2. Histology and weight comparison

Representative pictures of Hematoxylin & Eosin (H&E) stained liver sections of animals from the six different groups (A). At seven to nine days of age control mice weighed an average of 4.4g, while *Nlrp3*^{A350V} mice were significantly smaller. IL-17$^{-/-}$ mice were larger than *Nlrp3*^{A350V} IL-17$^{-/-}$ mice, while *Nlrp3*^{A350V} TNF$^{-/-}$ and TNF$^{-/-}$ mice were indistinguishable. Percent liver weight was significantly increased in *Nlrp3*^{A350V} mice when compared to control mice, the same pattern was observed in *Nlrp3*^{A350V} and IL-17$^{-/-}$ mice, while *Nlrp3*^{A350V} TNF$^{-/-}$ and TNF$^{-/-}$ showed a similar liver/body weight percentage (B). Severe liver inflammation – grade 3 - was present in *Nlrp3*^{A350V} mice and *Nlrp3*^{A350V}

IL-17$^{-/-}$ mice, while *Nlrp3*^{A350V} TNF$^{-/-}$ mice only showed mild inflammation (grade 1). (C) (* = $p<0.05$). Levels of IL1 β were increased in *Nlrp3*^{A350V} and Nlrp3^{A350V} IL-17$^{-/-}$ mice, but remained unchanged in Nlrp3^{A350V} TNF$^{-/-}$ compared to controls (D).

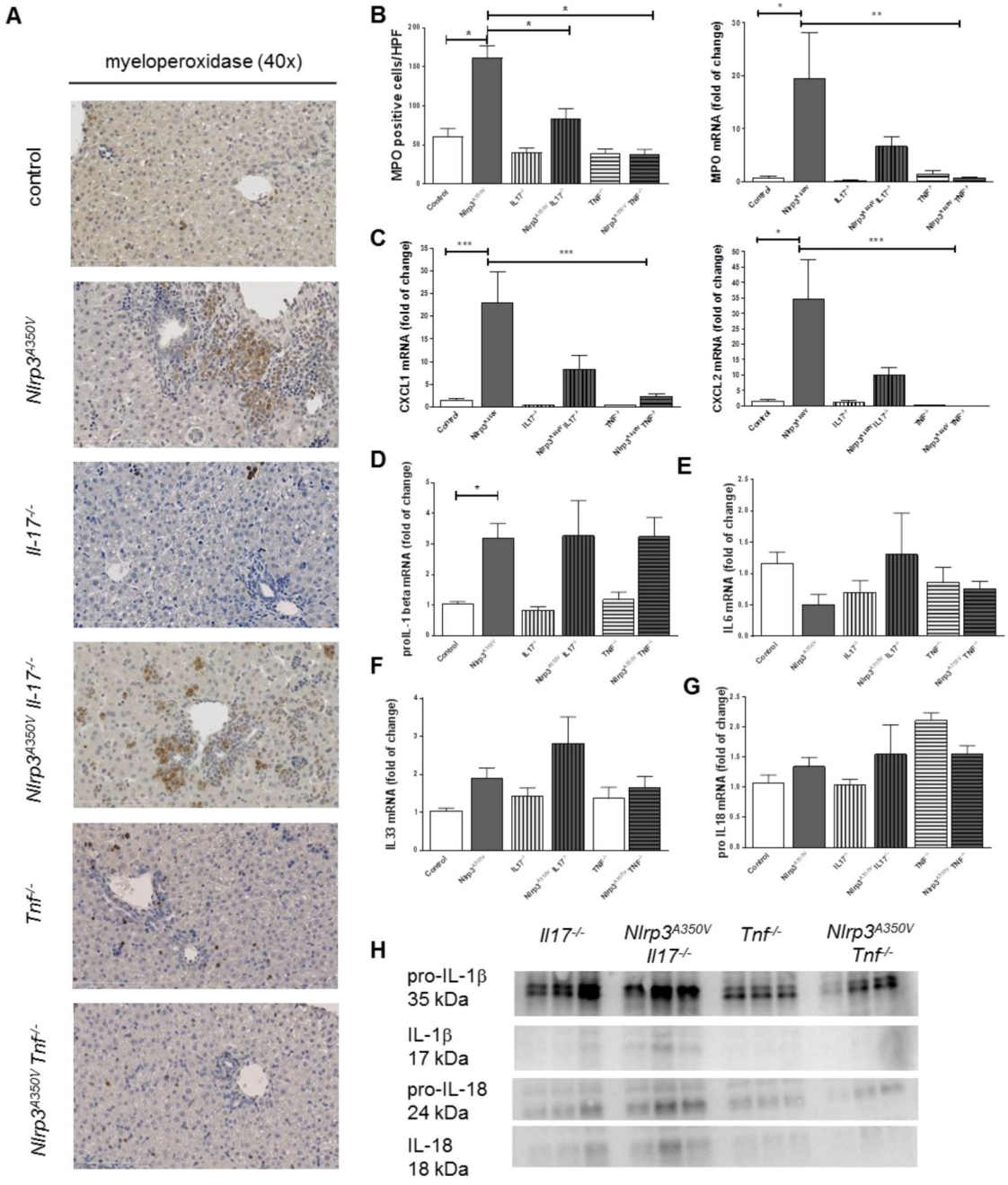

Figure 3. Regulation of neutrophilic infiltration, and proinflammatory cytokines

Immunohistochemistry for myeloperoxidase (MPO) showed increased staining in *Nlrp3*^{A350V} and *Nlrp3*^{A350V} IL-17$^{-/-}$, while the staining in livers of *Nlrp3*^{A350V} TNF$^{-/-}$ mice was not different from TNF$^{-/-}$ mice (A, B). mRNA levels of MPO were increased *Nlrp3*^{A350V} and *Nlrp3*^{A350V} IL-17$^{-/-}$ mice but not elevated in *Nlrp3*^{A350V} TNF$^{-/-}$ mice (B). As neutrophilic migration in mediated via chemokine ligands we quantified mRNA levels of CXCL1 and CXCL2 in livers. We found a marked increase of these chemokines in *Nlrp3*^{A350V} mice (20-fold for CXCL1 and 30-fold for CXCL2) when compared to control mice (C). This increase was also present in *Nlrp3*^{A350V} IL-17$^{-/-}$ mice (10-fold for CXCL1

and CXCL2) (C). pro-IL-1beta mRNA levels were upregulated in both Nlrp3^{A350V} TNF$^{-/-}$ mice and Nlrp3^{A350V} IL-17$^{-/-}$ mice compared to control mice (D), while all groups of mice displayed similar IL-6 (E), IL-33 (F) and pro-IL18 mRNA levels (G). However, protein levels of pro-IL1β and pro-IL18 as well as mature IL-1β and IL-18 were higher only in Nlrp3^{A350V} IL-17$^{-/-}$ but not in Nlrp3^{A350V} TNF$^{-/-}$ mice (H). (* = $p<0.05$; ** = $p<0.01$; *** = $p<0.001$).

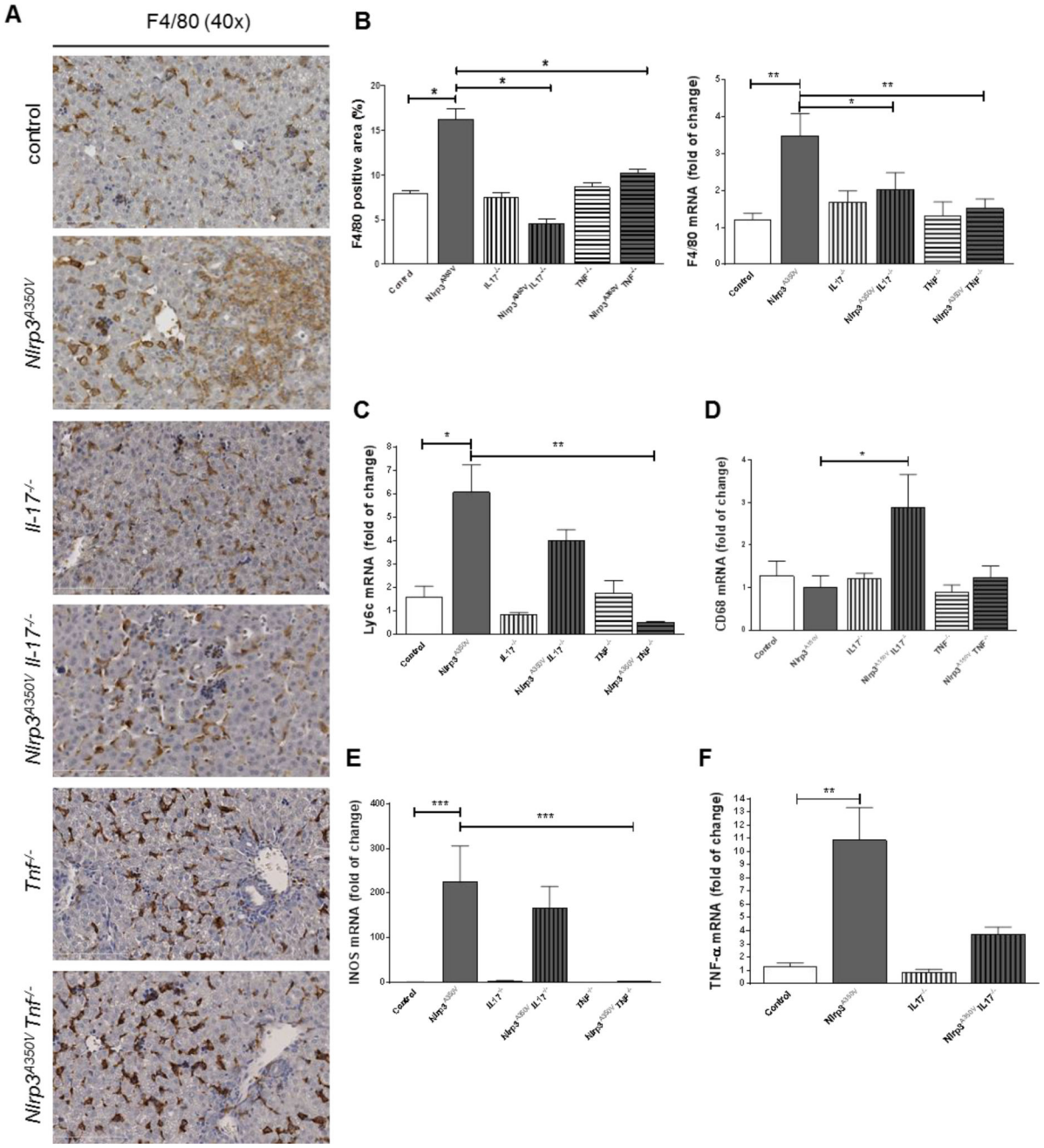

Figure 4. Macrophages infiltration and polarization in combined *Nlrp3*^{A350V} knockin and IL-17, TNF^{-} knockout mice

Hepatic macrophages when assessed via immunohistochemistry or mRNA levels for F4/80 were increased in *Nlrp3*^{A350V} mice and unchanged in all other groups of mice (A, B). Ly6-c mRNA levels were increased in Nlrp3^{A350V} mice and Nlrp3^{A350V} IL-17$^{-/-}$ mice but not in Nlrp3^{A350V} TNF$^{-/-}$ mice when compared to control mice (C). Surprisingly, CD68 mRNA levels were increased in *Nlrp3*^{A350V} IL-17$^{-/-}$ mice compared to *Nlrp3*^{A350V}, even though similar levels were found between mutant and control mice (D) The inflammatory phenotype of infiltrating macrophages in *Nlrp3*^{A350V} mice and *Nlrp3*^{A350V} IL-17$^{-/-}$ mice as

measured by mRNA levels of iNOS (inducible form of nitric oxide synthase) and TNF were found to be increased (E, F). (* = $p<0.05$; ** = $p<0.01$).

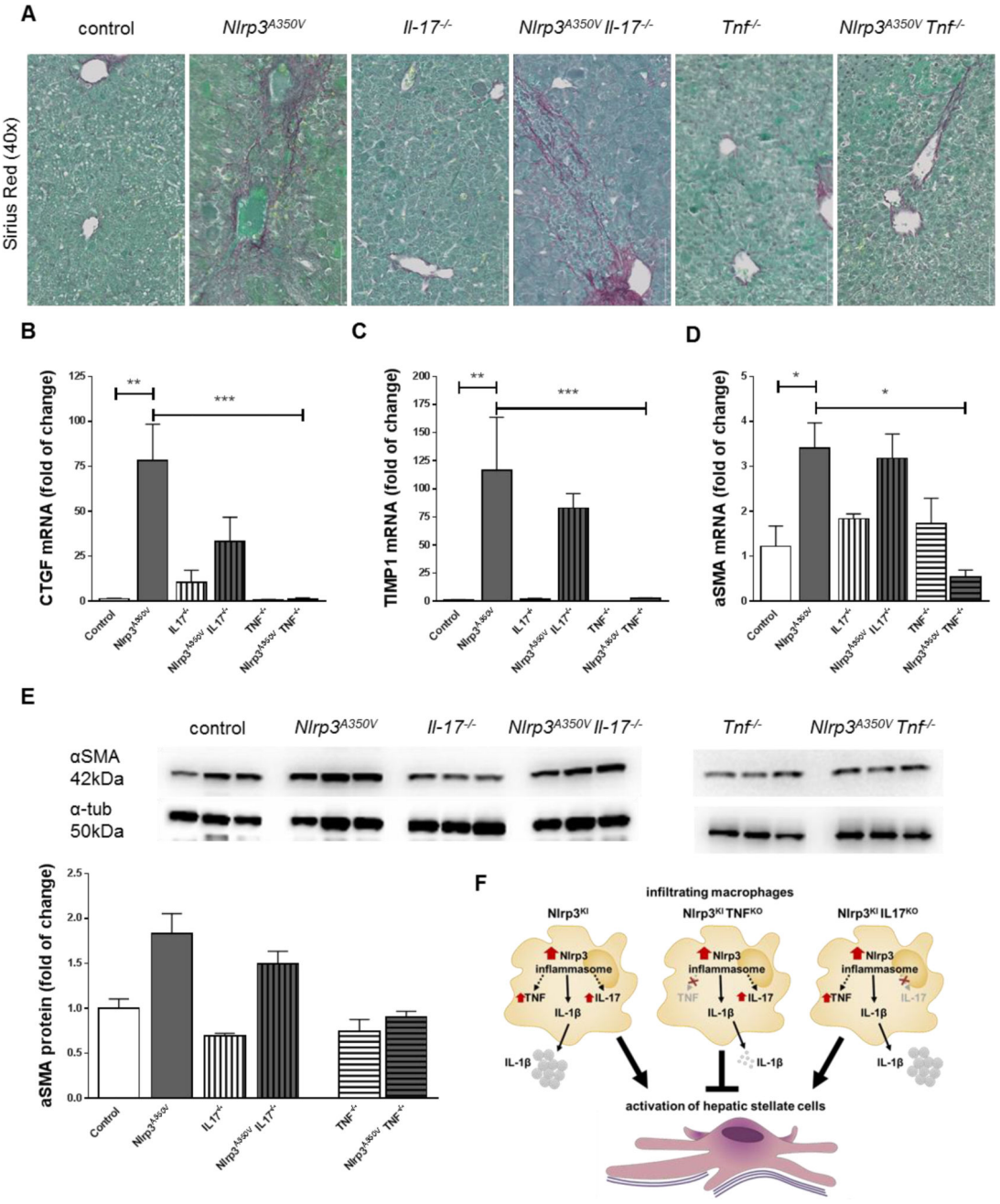

Figure 5. Collagen deposition and hepatic stellate cell activation in combined *Nlrp3*^{A350V} knockin and IL-17, TNF^{-} knockout mice

Sirius red staining uncovered bridging fibrosis in *Nlrp3*^{A350V} and *Nlrp3*^{A350V} IL-17$^{-/-}$, while control mice, IL-17$^{-/-}$, TNF$^{-/-}$, and *Nlrp3*^{A350V} TNF$^{-/-}$ only presented collagen deposition in close proximity to the portal fields (A). Markers for hepatic stellate cell (HSC) activation - connective tissue growth factor (CTGF), tissue inhibitor of matrix metalloproteinase 1 (TIMP1), and alpha smooth muscle actin (α-SMA) – were increased in *Nlrp3*^{A350V} and *Nlrp3*^{A350V} IL-17$^{-/-}$ mice when compared to control mice, while aforementioned markers were not increased in *Nlrp3*^{A350V} TNF$^{-/-}$ mice when compared to TNF$^{-/-}$ mice (B-D). Protein levels of α-SMA were also increased in *Nlrp3*^{A350V} and

Nlrp3^{A350V} IL-17$^{-/-}$ mice when compared to their corresponding control animals with no difference in *Nlrp3*^{A350V} TNF$^{-/-}$ and TNF$^{-/-}$ mice (E). Summary of the role of TNF and IL17 pathways in Nlrp3-driven liver damage (F) (* = $p<0.05$; ** = $p<0.01$; *** = $p<0.001$).

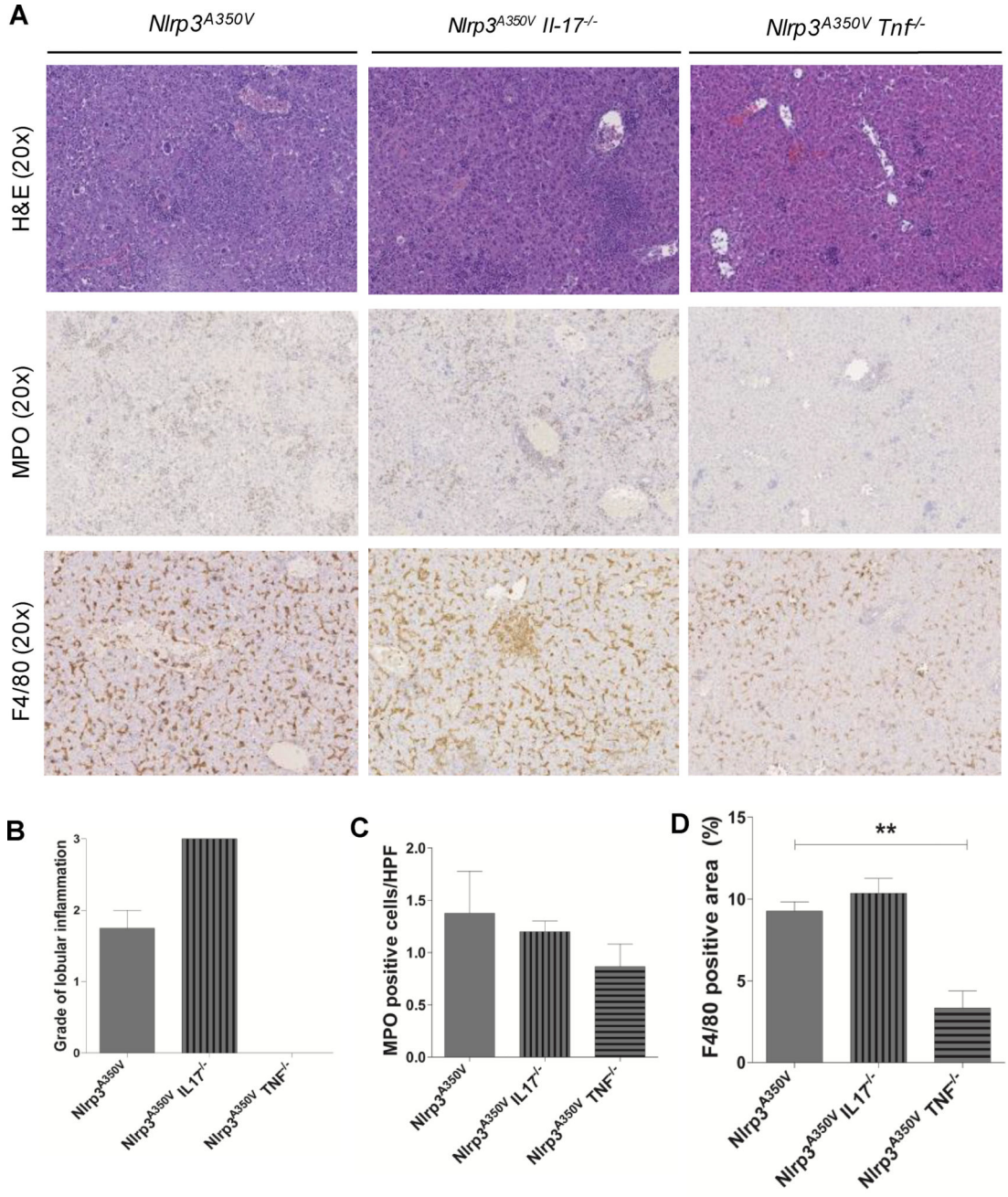

Figure 6. LPS-driven liver damage in combined *Nlrp3*^{A350V} knockin and IL-17, TNF^{-} knockout mice

Representative pictures of H&E, MPO, and F4/80 stained liver sections of animals from the three different groups after 4hr 25 μg/kg LPS injection (A). *Nlrp3*^{A350V} as well as *Nlrp3*^{A350V} *Il17*$^{-/-}$ mice exhibited severe liver inflammation (B) along with MPO positive cells infiltration (B) and the presence of high amount of F4/80 macrophages (D). *Nlrp3*^{A350V} Tnf$^{-/-}$ mice displayed a significant abrogation of liver inflammation as well as decreased numbers of MPO infiltrating cells and diminished amount of F4/80 positive cells (** = $p<0.01$).